Cholesterol differentially modulates the activity of opioid and muscarinic receptors via common non-canonical binding site

Nikolai Chetverikov, Alena Janoušková-Randáková, Dominik Nelic, and Jan Jakubík*

Institute of Physiology CAS, Prague, Czech Republic

*, corresponding author, jan.jakubik@fgu.cas.cz

Abstract

G protein-coupled receptors (GPCRs) are membrane proteins representing the largest and most therapeutically targeted receptor class for 30% of currently marketed drugs. Two binding motifs for membrane cholesterol, the 'cholesterol recognition amino acid consensus (CRAC) domain and 'cholesterol consensus motif' (CCM), were postulated. Using a simulation of molecular dynamics we demonstrate the binding of membrane cholesterol to non-canonical sites, distinct from CRAC and CCM, at muscarinic and opioid receptors. We identified a binding site common for muscarinic and opioid receptors at TM6, arginine 6.35 being the principal residue. Effects of depletion of membrane cholesterol on the functional responses of these receptors correlated with effects of mutations arginine 6.35 on functional responses. Exploiting cholesterol-binding sites and variations in receptor-membrane interactions brings novel pharmacotherapeutic opportunities including tissue-specific targeting for sterol-based modulators.

Introduction

G protein-coupled receptors (GPCRs) are receptors that mediate diverse physiological functions. Over 800 members of the GPCR superfamily comprise the largest and most therapeutically targeted receptor class representing 30% of currently marketed drugs[1]. Cholesterol has been found co-crystallised with many GPCRs[2]. Membrane cholesterol allosterically modulates ligand binding to and activation of GPCRs and affects the pharmacology of GPCRs[3]. Cholesterol content varies among tissues. For example, neurons contain higher cholesterol than smooth muscle cells. This suggests that membrane cholesterol affects GPCR signalling in various tissues to a different extent. Thus, variation in interactions of receptors with the membrane represents a possibility to achieve pharmacological selectivity based on differences in membrane composition. This affords achieving tissue-specific selectivity according to the cholesterol content of a given tissue.

Two binding motifs for membrane cholesterol were postulated. First, the so-called 'cholesterol recognition amino acid consensus (CRAC) domain common for all membrane proteins that contain a (–L/V-(X)1–5-Y-(X)1–5-R/K-) pattern was described[4]. Subsequently a (K/R)-X1−5-(Y/F)-X1−5-(L/V) reversed pattern (CARC) was found in the nicotinic acetylcholine receptor[5]. The so-called 'cholesterol consensus motif' (CCM) was identified in the structure of the β_2-adrenergic receptor (3D4S) and predicted for a plethora of other GPCRs[6]. Yet, a current extensive study of cryo-EM and X-ray structures has shown that almost all cholesterol binding to GPCRs occurs in predictable locations that, however, lack perceivable cholesterol-binding motifs[7]. In our previous study, we have shown that membrane cholesterol prevents persistent activation of muscarinic receptors by wash-resistant xanomeline by interaction with $R^{6.35}$ and $L/I^{6.46}$(Ballesteros and Weinstein numbering[8] in the TM6[9]. The identified cholesterol-binding site does not correspond to any known cholesterol-binding motif.

Similarly to M_2 and M_4 muscarinic receptors, a substantial number of $G_{i/o}$-coupled class A GPCRs possess a basic residue in position 6.35 and hydrophobic L/I/V in position 6.46 next to a conserved proline kink (Supplementary Information, Figure S1). We speculate that membrane cholesterol also binds to $R^{6.35}$ at opioid receptors. In the presented study we docked cholesterol to M_2 and M_4

muscarinic receptors and δ-, κ- and μ-opioid receptors by simulation of molecular dynamics. We identified two common cholesterol-binding sites including the one containing $R^{6.35}$.

Results

Coarse-grained molecular dynamics

To identify potential cholesterol-binding sites at muscarinic and opioid receptors, coarse-grained molecular dynamics (cgMD) of a 20 nm x 20 nm patch of membrane containing 30% of cholesterol molecules and one receptor was simulated. Throughout cgMD cholesterol molecules associated with the receptor and remained bound to it for hundreds of nanoseconds (Supplementary Information SI Figure 2 to 4). To verify the approach, structures of the β_2-adrenergic receptor (3D4S) and A_{2A}-adenosine receptor (5IU4) were included in the test set. Cholesterol in locations appearing in these crystal structures was observed, validating the method (Supplementary Information Figure S2). Namely, binding to the cholesterol consensus motif (CCM) between TM2 and TM4 of the β_2-adrenergic receptor and TM2-TM3-TM4 extracellular bundle and TM6 extracellular part of the A_{2A}-adenosine receptor was observed. Subsequently, cgMD was run at δ-opioid (4EJ4), κ-opioid (4DJH), μ-opioid (4DKL), M_2-muscarinic (3UON) and M_4-muscarinic (5DSG) receptors in an inactive conformation and δ-opioid (6PT2), κ-opioid (6B73) and μ-opioid (5C1M), M_2-muscarinic (4MQS) and M_4-muscarinic (8FX5) receptors in an active conformation. We have observed up to five concurrently bound molecules of cholesterol to seven unique binding sites (Supplementary Information Figure S3 and S4).

Cholesterol re-docking

Seven unique cholesterol-binding sites on muscarinic and opioid receptors were identified using cgMD, three in the extracellular and four in the intracellular leaflet of the membrane (Figure 1). Cholesterol molecules in the extracellular leaflet interacted with TM1-TM2-TM7 (e1-e2-e7) bundle of helices or groove between TM4-TM5 (e4-e5) or TM6-TM7 (e6/e7) helices. Cholesterol molecules in the intracellular leaflet interacted with the TM1-TM2-TM4 (i1-i2-i4) bundle of helices or groove between TM3-TM4 (i3-i4), TM5-TM6 (i5-i6) or TM6-TM7 (i6-i7) helices or with TM7 (i7) helix. Specifically, cholesterol bound to four sites (e1-e2-e7, e6-e7, i3-i4 and i6-i7) at δ- and κ-opioid receptors, five sites (e1-e2-e7, e6-e7, i5-i6, i6-7 and i7) at the μ-opioid receptor (Supplementary Information Figure S5) and six sites (e1-e2-e7, e4-e5, i3-i4, i5-i6, i6-i7 and i7) at muscarinic receptors (Supplementary Information Figure S6). Individual molecules of cholesterol were back-mapped onto the receptor and re-docked and rescored. Re-docking binding energy estimates were above 4 kcal/mol. Two binding sites were common for all studied receptors: e1-e2-e7 and i6-i7. Hydrogen bonding to $R^{6.35}$ was common to all receptors in at least one conformation. Binding to the e1-e2-e7 sites markedly varied among receptors.

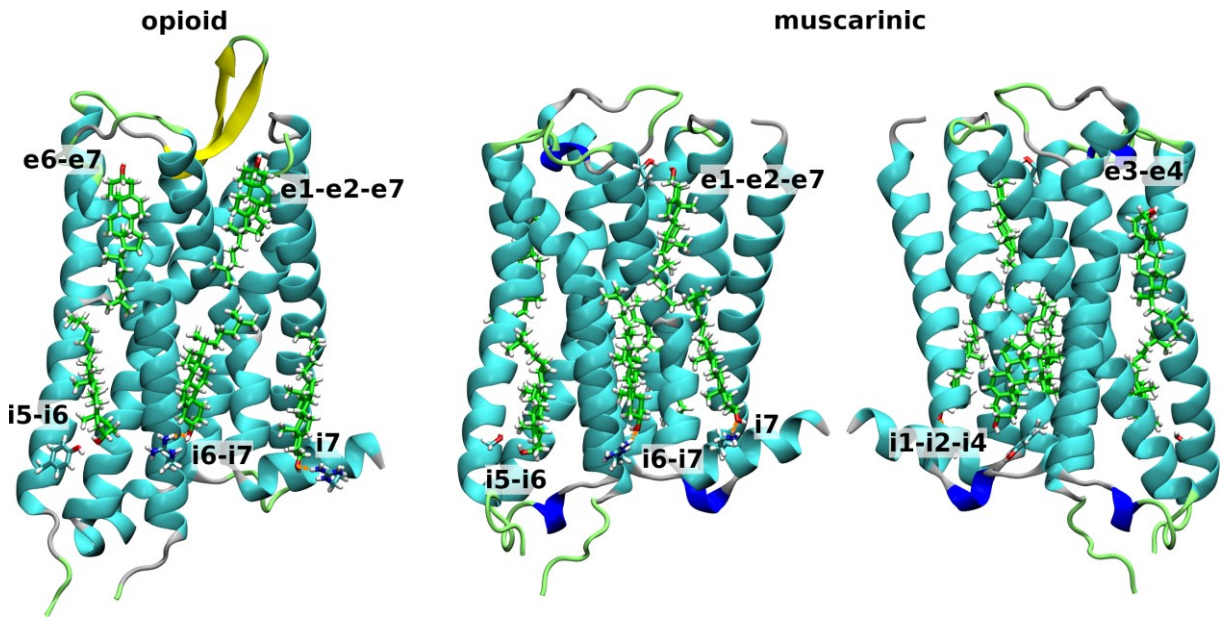

Figure 1 Cholesterol binding to opioid and muscarinic receptors
Molecules of cholesterol that associated with the opioid (left) or muscarinic receptor (middle and right) were back-mapped and re-docked to the receptor. Orientation: extracellular up, TM6 front (left and middle) or TM4 front (right). Cholesterol (green carbons) in the extracellular leaflet interacting with TM1-TM2-TM7 (e1e2-e7) bundle or TM3-TM4 (e3-e4) or TM6-TM7 (e6-e7) groove and in the intracellular leaflet interacting with TM1-TM2-TM4 (i1-i2-i4) bundle or TM5-TM6 (i5-i6) or TM6-TM7 (i6-i7) groove or TM7 (i7) helix is shown.

Conventional molecular dynamics

The complexes of receptors and re-docked individual molecules of cholesterol were subjected to three replicas of conventional MD (cMD). Analysis of cMD trajectories revealed various degrees of the stability of bound cholesterol. The quantitative analysis of interactions between receptor and cholesterol molecules is in Figure 2. The principal receptor residues interacting with cholesterol are listed in Table 1. Receptor activation led to changes in cholesterol binding to the receptors.

Opioid receptors

Four unique cholesterol-binding sites were identified on the δ-opioid receptor (Table 1, Supplementary information Figure S5). Binding to e6-e7 and i3-i4 sites was similar for receptors at inactive and active conformations, respectively. In the e6-e7 site, the cholesterol binding was mediated by hydrophobic interaction with F280$^{6.54}$ (superscript, Ballesteros-Weinstein numbering[8]). Cholesterol binding to the i3-i4 site was weak at both conformations. In an inactive conformation (4EJ4), binding was mediated by hydrophobic interactions with F137$^{3.41}$. In an active conformation (6PT2), binding was mediated by hydrogen bonding to K155$^{3.59}$. While cholesterol binding to the e1-e2-e7 site at an inactive conformation was primarily mediated by hydrophobic interaction with L295$^{7.30}$, at an active conformation it was mediated by hydrogen bonding to S44$^{1.27}$. Cholesterol binding to the i6-i7 site of the δ-opioid receptor was via hydrogen bond to R261$^{6.35}$ that was more frequent in an active conformation than in an inactive conformation. In an active conformation, cholesterol was shifted towards TM7 interacting with F320$^{7.55}$.

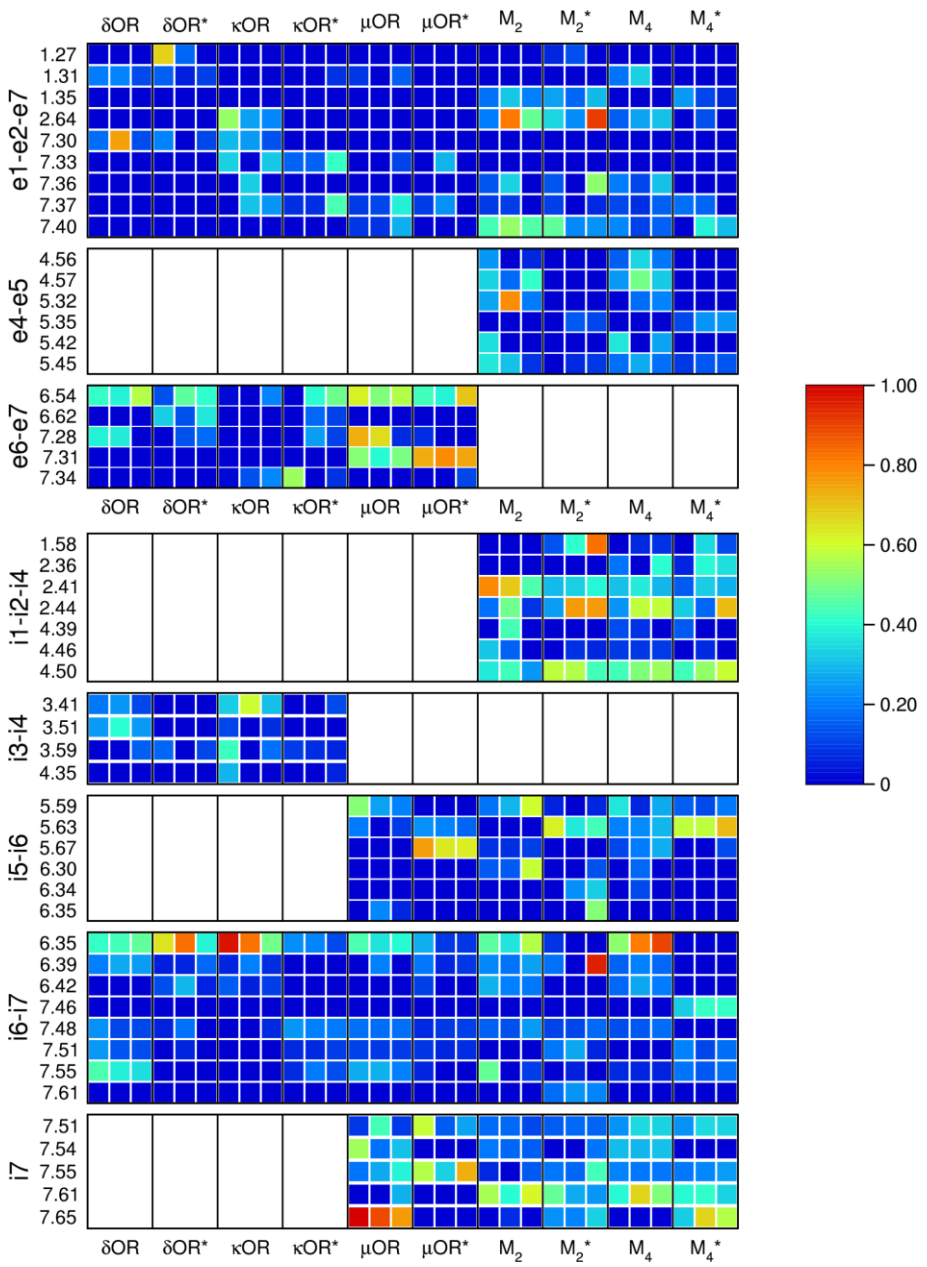

Figure 2 Interactions between cholesterol and receptor

Histograms of interactions between receptors indicated on x-axis and cholesterol molecules in the extracellular leaflet interacting with e1-e2-e7 bundle, e4-e5 groove or e6-e7 groove and in the intracellular leaflet interacting with i1-i2-i4 bundle, i3-i4 groove, i5-i6 groove, i6-i7 groove or i7 helix indicated on y-axis were calculated from MD trajectories using Ligand Interaction Diagram in Maestro. Only residues interacting with cholesterol at more than 20% of time-frames in at least one MD replica are displayed. Each square represents one of 3 independent MD replicas. Values over 1.0 are possible as some protein residues may make multiple contacts with cholesterol within one timeframe. However, no values greater than 1 were obtained.

Similar to the δ-opioid receptor, four unique cholesterol-binding sites were identified on the κ-opioid receptor (Table 1, Supplementary Information Figure S5). In contrast to the δ-opioid receptor, however, cholesterol binding to the extracellular e1-e2-e7 site was more frequent at an inactive conformation (4DJH) than at an active conformation (6B73). In an inactive conformation, it was mediated by frequent hydrogen bonding with Y119$^{2.64}$ and S310$^{7.33}$, and in an active conformation by less-frequent hydrogen bonding with S310$^{7.33}$ only. Cholesterol binding to the e6-e7 site was mediated

by hydrogen bonding to S311$^{7.34}$ and hydrophobic integrations with F293$^{6.54}$ that were more frequent in an active than inactive conformation. Cholesterol binding to the i3-i4 site of the receptor in an inactive conformation was mediated by F147$^{3.41}$ and K165$^{3.59}$. At the receptor in an active conformation, cholesterol binding was weak and cholesterol dissociated from the binding site. In the i6 site, the cholesterol binding was primarily mediated via a hydrogen bond with R274$^{6.35}$, which was more frequent at an active conformation than an inactive one.

Five unique cholesterol-binding sites were identified on the μ-opioid receptor (e1-e2-e7, e6-e7, i3-i4, i6-i7, i7), three being common with δ- and κ-opioid receptors (Table 1, Supplementary Information Figure S5). The strongest cholesterol binding was identified at the i7 site. In an inactive conformation (4DKL), cholesterol binding to the i7 site was mediated by R348 in the Helix8. In an active conformation (5C1M), cholesterol binding to the i7 site was mediated by V334$^{7.51}$ and F338$^{7.55}$. The cholesterol binding to the i7 site was more frequent to an inactive conformation than to an active one. Also binding to the e6-e7 site was relatively strong. It was mediated by hydrophobic interaction with Y299$^{6.54}$ and hydrogen bonding to Q314 in the third extracellular loop. At inactive conformation, hydrogen bonding to Q314 was less frequent in expense for hydrogen bonding to T311$^{7.28}$. Cholesterol binding to the i5-i6 site was mediated by hydrogen bonding to K260 in the third intracellular loop of an active conformation or less frequent binding to Y252$^{5.59}$ in the TM5 helix of an inactive conformation. Like at other tested receptors, cholesterol binding to the i6-i7 site was mediated via a hydrogen bond with R280$^{6.35}$, interacting more frequently with it at an inactive conformation. In an inactive conformation, cholesterol binding was further stabilised by hydrophobic interactions with TM7 via L331$^{7.48}$ and F338$^{7.55}$.

Muscarinic receptors

Six unique cholesterol-binding sites were identified on muscarinic receptors (Table 1, Supplementary Information Figure S6). Integration patterns of M_2 and M_4 receptors were similar. The most profound differences between inactive and active conformations were observed for cholesterol binding to the e4-e5 and i6-i7 sites (Figure 2). In an inactive conformation of the M_2-muscarinic receptor (3UON) cholesterol at the e4-e5 site primarily interacted with W155$^{4.57}$ and T190$^{5.42}$. Identically in an inactive conformation of the M_4-muscarinic receptor (5DSG) cholesterol primarily interacted with W164$^{4.57}$ and T199$^{5.42}$. In active conformations (M_2 4MQS; M_4 8FX5), these principal interactions were missing as cholesterol binding was unstable. Like opioid receptors, cholesterol binding to the i6-i7 site of the M_2 and M_4 receptors in inactive conformations was mainly mediated by hydrogen bonding to R387$^{6.35}$ and R354$^{6.35}$, respectively. In active conformations, cholesterol moved towards Helix8 and bound to K448 of M_2 or R400 of M_4 receptor. Cholesterol binding to the e1-e2-e7 site of the M_2 receptor in an inactive conformation was mainly mediated by Y84$^{2.64}$ and W427$^{7.40}$. In an active conformation, these interactions persisted but bonding to W427$^{7.40}$ was about 5 times less frequent. Cholesterol binding to the e1-e2-e7 site of the M_4 receptor was in principle the same but much weaker and at an inactive conformation of the receptor unstable. Cholesterol binding to the i1-i2-i4 site of the M_2 and M_4 receptors was strong. At M_2-receptor cholesterol binding was mainly mediated by Y60$^{2.41}$, F63$^{2.44}$, T237$^{4.39}$ and W148$^{4.50}$ at an inactive conformation and K49$^{1.58}$, Y60$^{2.41}$, F63$^{2.44}$ and W148$^{4.50}$ at an active conformation. At M_4-receptor cholesterol binding to the i1-i2-i4 site was mainly mediated by F63$^{2.44}$ and W148$^{4.50}$ at both conformations. Cholesterol binding to the i5-i6 site of the M_2 receptor was mainly mediated by Y206$^{5.58}$ and E382$^{6.30}$ at an inactive conformation and by S210$^{5.63}$, T386$^{6.34}$ at an active conformation. In an active conformation, cholesterol moves towards R387$^{6.35}$ and forms hydrogen bonds with it. Cholesterol binding to the i5-i6 site of the M_4 receptor was mainly mediated by S219$^{5.63}$ at both conformations. Cholesterol binding to the i7 site was mediated by hydrogen bonding to lysine (M_2 K448, M_4 K415)in Helix 8 at both active and inactive conformations. At active conformations, it moves further from the TM7 helix and forms a hydrogen bond with K452 (M_2) or R419 (M_4).

Table 1 - Principal residues interacting with cholesterol during conventional MD
Principal residues of interaction between receptor (the first column) and cholesterol molecule in the extracellular leaflet interacting with TM1-TM2-TM7 (e1-e2-e7) bundle or TM4-TM5 (e4-e5) or TM6-TM7 (e6-e7) groove and in the intracellular leaflet interacting with TM1-TM2-TM4 (i1-i2-i4) bundle or TM3-TM4 (i3-i4), TM5-TM6 (i5-i6) or TM6-TM7 (i6-i7) groove or TM7 (i7) helix throughout MD trajectory are listed. Superscript, Ballesteros-Weinstein numbering; ECL3, the third extracellular loop; ICL3, the third intracellular loop.

Structure	e1-e2-e7	e4-e5	e6-e7	i1-i2-i4	i3-i4	i5-i6	i6-i7	i7
δ-OR 4EJ4 inactive	L295$^{7.30}$		F280$^{6.54}$ D293$^{7.28}$		F137$^{3.41}$ Y147$^{3.51}$		R261$^{6.35}$ V265$^{6.39}$ F320$^{7.55}$	
δ-OR 6PT2 active	S44$^{1.27}$		F280$^{6.54}$ D288$^{6.62}$		K155$^{3.59}$		R261$^{6.35}$ G268$^{6.42}$	
κ-OR 4DJH inactive	Y119$^{2.64}$ S310$^{7.33}$ Y313$^{7.36}$ F314$^{7.37}$		F293$^{6.54}$ S311$^{7.34}$		F147$^{3.41}$ K165$^{3.59}$		R274$^{6.35}$	
κ-OR 6B73 active	S310$^{7.33}$ F314$^{7.37}$		F239$^{6.54}$ S305$^{7.28}$ S311$^{7.34}$				R274$^{6.35}$ L325$^{7.48}$ F332$^{7.55}$	
μ-OR 4DKL inactive	F320$^{7.37}$ A323$^{7.40}$		Y299$^{6.54}$ T311$^{7.28}$ Q314^{ECL3}			Y252$^{5.59}$	R280$^{6.35}$ L331$^{7.48}$ F338$^{7.55}$	V334$^{7.51}$ A337$^{7.54}$ R348^{Helix8}
μ-OR 5C1M active	S317$^{7.33}$ F320$^{7.37}$		Y299$^{6.54}$ Q314^{ECL3}			I256$^{5.63}$ K260^{ICL3}	R280$^{6.35}$	V334$^{7.51}$ F338$^{7.55}$
M_2 3UON inactive	I26$^{1.35}$ Y84$^{2.64}$ W427$^{7.40}$	W155$^{4.57}$ F180$^{5.32}$ T190$^{5.42}$		Y60$^{2.41}$ F63$^{2.44}$ T137$^{4.39}$ W148$^{4.50}$		Y206$^{5.58}$ E382$^{6.30}$	R387$^{6.35}$ A391$^{6.39}$ L394$^{6.42}$ L442$^{7.55}$	K448^{Helix8}
M_2 4MQS active	I26$^{1.35}$ Y84$^{2.64}$ W427$^{7.40}$			K49$^{1.58}$ Y60$^{2.41}$ F63$^{2.44}$ W148$^{4.50}$		S210$^{5.63}$ T386$^{6.34}$ R387$^{6.35}$	A391$^{6.39}$ A438$^{7.51}$ K448^{Helix8}	L442$^{7.55}$ K448^{Helix8} K452^{Helix8}
M_4 5DSG inactive	E31$^{1.31}$ Y92$^{2.64}$ S290$^{7.36}$	W164$^{4.57}$ T199$^{5.42}$		F72$^{2.44}$ W157$^{4.50}$		S219$^{5.63}$	R354$^{6.35}$	A405$^{7.51}$ A408$^{7.54}$ K415^{Helix8}
M_4 8FX5 active	F34$^{1.35}$ W440$^{7.40}$			F72$^{2.44}$ W157$^{4.50}$		S219$^{5.63}$	R400$^{7.46}$	K415^{Helix8} R419^{Helix8}

Common features of cholesterol binding

Taken together, the sites e1-e2-e7 and i6-i7 were detected in all structures (Figure 2, Supplementary Information Figure S5 and S6). Cholesterol binding to the e1-e2-e7 bundle varied among receptor families and subtypes. Cholesterol binding to the e1-e2-e7 bundle was weak at μ-opioid and M_4-muscarinic receptors. Cholesterol binding to e1-e2-e7 bundle was mediated mainly by Y$^{2.64}$ at

M_2-muscarinic and κ-opioid receptors, by $L^{7.30}$ at δ-opioid receptor in an inactive conformation and $S^{1.27}$ at δ-opioid receptor in an active conformation. The principal interaction residue of cholesterol binding to the i6-i7 groove was $R^{6.35}$. Cholesterol binding to $R^{6.35}$ was much more frequent at inactive than active conformations of M_2, M_4, κ and μ receptors (Figure 2). In contrast, cholesterol binding to $R^{6.35}$ was more frequent to an active conformation than to an inactive conformation of δ-opioid receptor.

Functional responses – membrane-cholesterol depletion

To assess the effects of membrane cholesterol on the functional response of muscarinic and opioid receptors, membrane cholesterol was depleted in CHO cells expressing individual receptor subtypes by treatment with methyl-β-cyclodextrin (MβCD). The treatment lowered the concentration of membrane cholesterol from 225 ± 22 to 85 ± 13 nmol/mg of protein. The functional response of M_2-, M_4-muscarinic, δ-, κ- and μ-opioid receptors was measured as stimulation of [^{35}S]GTPγS binding to membranes prepared from CHO cells by the agonists carbachol (muscarinic), Leu-enkephalin (δ- and κ-opioid) or endomorphin I (μ-opioid receptors). After subtraction of non-specific binding, [^{35}S]GTPγS binding was normalized to total GTPγS binding sites. The effects of cholesterol depletion varied among receptors. Cholesterol depletion changed basal GTPγS binding (% of total GTPγS binding sites in the absence of an agonist) to membranes, increasing it at M_2- and M_4-muscarinic receptors (Figure 3, red and turquoise) and decreasing it at δ- and μ-opioid receptors (Figure 3, yellow and blue). Basal GTPγS binding to membranes expressing κ-opioid receptors remained unchanged. Membrane-cholesterol depletion increased maximum GTPγS binding at both muscarinic receptors and decreased maximum GTPγS binding at all opioid receptors. Membrane-cholesterol depletion decreased the half-efficient concentration EC_{50} at both muscarinic and μ-opioid receptors and increased it at κ-opioid receptor. EC_{50} was not affected at δ-opioid receptors (Supplementary Information Table S1).

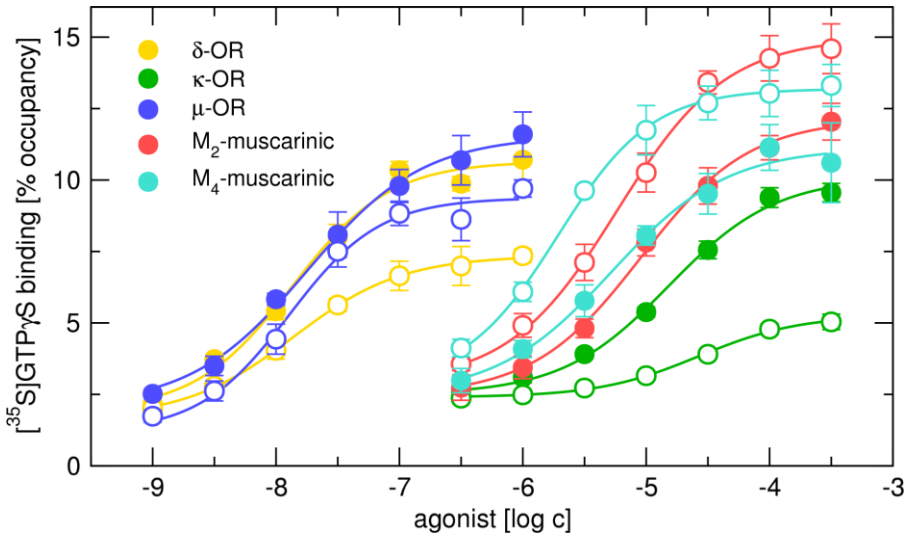

Figure 3 Effects of membrane-cholesterol depletion on functional response to agonists
Effects of membrane-cholesterol depletion (open symbols) on functional responses of δ- (yellow), κ-opioid (green) receptors to Leu-enkephalin, μ-opioid receptors (blue) to endomorphin I and M_2- (red) and M_4-muscarinic (turquoise) receptors to carbachol. Ordinate, [^{35}S]GTPγS binding is expressed as % of occupancy of G-protein binding sites. Abscissa, the concentration of agonist is expressed as a decadic logarithm of molar concentration. Data are means ± SD from 3 independent experiments performed in quadruplicates.

Functional responses – mutations

As cholesterol binds to the i6-i7 groove at all investigated receptors and $R^{3.65}$ plays a key role in cholesterol binding at the majority of them, R6.35 was mutated to either alanine (neutral mutation) or glutamate (reverse charge mutation) found in some receptors (Supplementary information Figure S1). Again, the functional response of M_2- and M_4-muscarinic and δ-, κ- and μ-opioid receptors was measured as stimulation of [^{35}S]GTPγS binding to membranes prepared from CHO cells by the agonists carbachol (muscarinic), Leu-enkephalin (δ- and κ-opioid) or endomorphin I (μ-opioid receptors). Similarly to cholesterol depletion, mutations of $R^{6.35}$ differentially affected the functional responses of studied receptors. Both mutations increased basal binding (in the absence of an agonist) of GTPγS binding to M_2- and M_4-muscarinic receptors (Figure 4, red and turquoise) and decreased basal GTPγS binding at δ- and μ-opioid receptors (Figure 4, yellow and blue). None of the mutations affected basal GTPγS binding to membranes expressing κ-opioid receptors (Figure 4, green). Both mutations increased maximum GTPγS binding at both muscarinic receptors and decreased maximum GTPγS binding at κ-opioid receptor. Mutation of $R^{6.35}$ to glutamine decreased E_{MAX} at μ-opioid receptor. Mutations of R6.35 to alanine did not affect E_{MAX} at this receptor. Both mutations decreased EC_{50} values at both muscarinic and κ-opioid receptors. EC_{50} was not affected at δ- and μ-opioid receptors by these mutations (Supplementary Information Table S2).

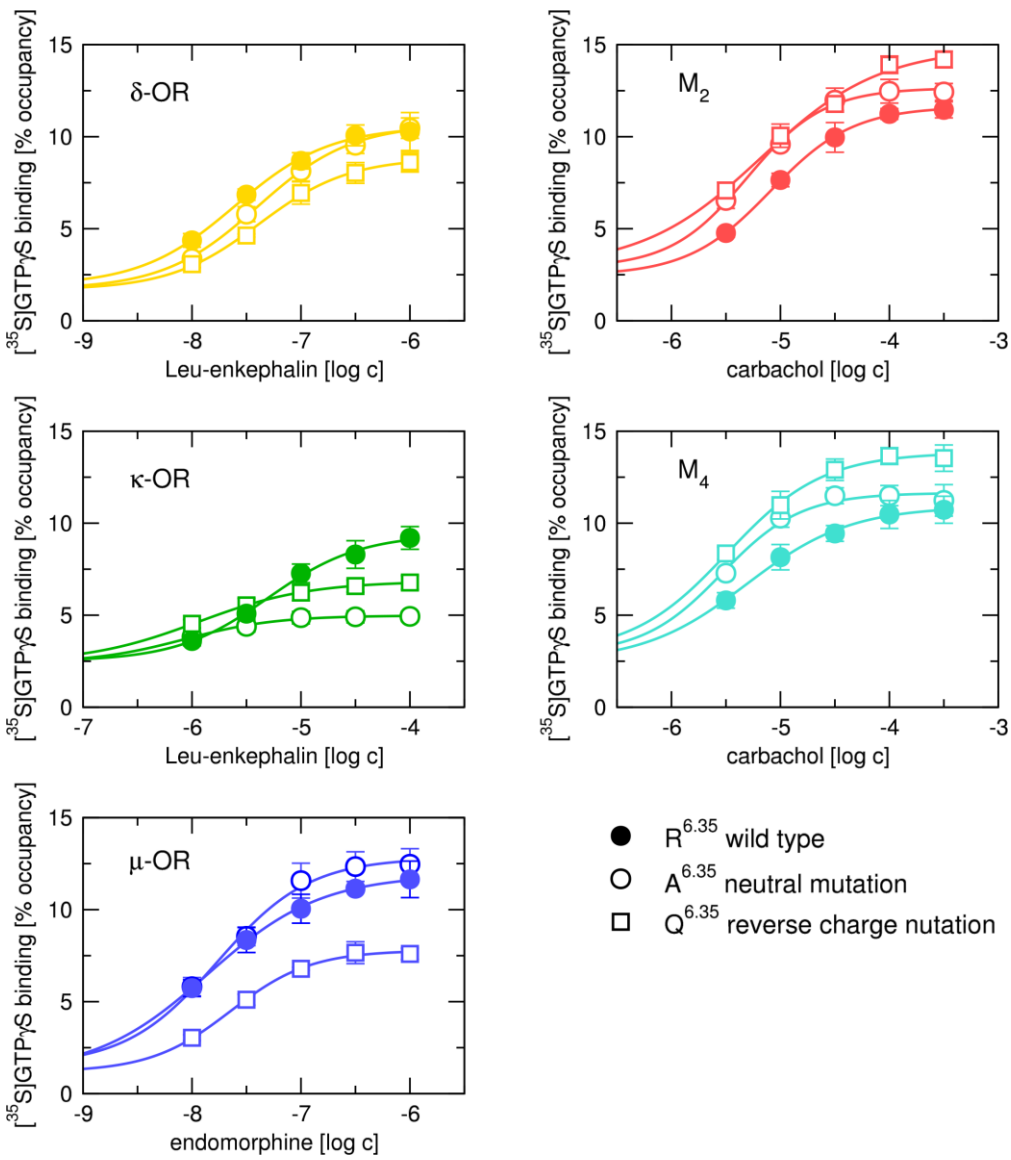

Figure 4 Effects of mutation of $R^{6.35}$ on functional response to agonists
Effects of mutations of wild type $R^{6.35}$ (full symbols) to alanine (neutral mutation, open circles) or glutamine (reverse charge mutation, open squares) on functional responses of δ- (yellow), κ-opioid (green) receptors to Leu-enkephalin, μ-opioid receptors (blue) to endomorphin I and M_2- (red) and M_4-muscarinic (turquoise) receptors to carbachol. Ordinate, [^{35}S]GTPγS binding is expressed as % of occupancy of G-protein binding sites. Abscissa, the concentration of agonist is expressed as a decadic logarithm of molar concentration. Data are means ± SD from 3 independent experiments performed in quadruplicates.

Overall, the effects of mutations on basal GTPγS binding were the same as the effects of cholesterol depletion. Also, the effects of mutations on E_{MAX} and EC_{50} at muscarinic receptors were the same as the effects of cholesterol depletion. In contrast, cholesterol depletion strongly decreased E_{MAX} of functional response of mutated M_2- and M_4-muscarinic receptors, having the opposite effect in comparison to wild-type receptors (Supplementary Information Figure S7 and Table S3), indicating additional mechanism by which cholesterol affects functional properties of muscarinic receptors.

Discussion

Membrane cholesterol allosterically modulates ligand binding to and activation of GPCRs and affects the pharmacology of GPCRs[3]. Three cholesterol-binding motifs were postulated[4–6]. However, the majority of cholesterol binding in cryo-EM and X-ray structures of GPCRs occurs in the sites not conforming to these binding motifs[7]. In the present study, we show cholesterol binding to such a non-canonical site at TM6 of muscarinic and opioid receptors. The binding to this site is primarily mediated by hydrogen bonding to $R^{6.35}$ (Figure 1 and Figure 2).

Cholesterol was docked to GPCRs by simulation of molecular dynamics. The procedure successfully identified all cholesterol-binding sites observed in the X-ray structures of the β_2-adrenergic receptor (3D4S)[6] and A_{2A}-adenosine receptor (5IU4)[10] (Supplementary information Figure S2). Eight unique cholesterol-binding "domains" on muscarinic and opioid receptors were identified (Figure 1, Table 1). Two of them were common for muscarinic and opioid receptors. At opioid receptors, observed cholesterol binding in the extracellular leaflet to TM6-TM7 groove (e6-e7 site) corresponds to cholesterol co-crystallized in structures 4DKL, 5C1M, 6PT2 and 6B73 further validating the procedure[11–14]. Cholesterol did not appear in the X-ray or cryo-EM structures of muscarinic receptors. However, the observed binding of cholesterol in the intracellular leaflet to the TM1-TM2-TM4 bundle (i1-i2-i4 site) corresponds to cholesterol hemisuccinate appearing in X-ray (5CXV) and cryo-EM (6OIJ) structures of the M_1-muscarinic receptor[15, 16]. The binding of cholesterol to receptors in active conformations diverged from its binding to receptors in inactive conformations, indicating a modulatory role of membrane cholesterol on receptor activation. Major differences in binding to active versus inactive conformation were observed for the i6-i7 site for all receptors. Depletion of membrane cholesterol differentially modulated activation of muscarinic and opioid receptors (Figure 3). Depletion of membrane cholesterol augmented activation of both muscarinic receptors and diminished to various extent activation of all opioid receptors. These findings agree with previous observations[17]. Effects of mutations of $R^{6.35}$ to glutamine on functional response to agonists were similar to the effects of cholesterol depletion, suggesting these mutations impair cholesterol binding to $R^{6.35}$. Thus i6-i7 groove appears to be a non-canonical cholesterol binding site through which cholesterol differentially modulates the functional response of studied receptors.

Cholesterol-mediated receptor oligomerisation via the TM6-TM7 interface was modelled for dimers of muscarinic receptors[18]. The position of cholesterol molecules in the model was given by template structures of β_2-adrenergic and 5-HT_{2B}-serotonin receptors. Binding to the e6-e7 site was not confirmed by the presented study for muscarinic receptors but was found at opioid receptors (Table

1**Error! Reference source not found.**). This may be given by the orientation of polar and acidic residues in the extracellular edge of TM6 and TM7 of muscarinic receptors out of the membrane, preventing their interaction with the hydroxy group of cholesterol.

Understanding molecular mechanisms of cholesterol binding to GPCRs appears to be important as modulation of GPCRs from the cholesterol-binding site offers several therapeutic opportunities. At muscarinic receptors, a cholesterol-binding site was shown to bind neuroactive steroids[19]. Thus, neurosteroids and steroid hormones modulating muscarinic receptors[20–22] very likely act via cholesterol-binding sites. The neurosteroid pregnanolone sulphate has been shown to increase acetylcholine release in the frontal cortex, amygdala and hippocampus and improve spatial recognition[23, 24]. The steroid whitanone blocked the negative effects of scopolamine on cholinergic signalling, exerted neuroprotective effects and promoted neuroregeneration and memory recovery[25, 26]. Like muscarinic receptors, membrane cholesterol affected the binding and function of opioid receptors[17]. Membrane cholesterol modulated the partitioning of δ-opioid receptors to membrane rafts[27]. Also, the binding of steroids to opioid receptors affecting their functional response was observed[28, 29]. Steroid activating μ-opioid receptors was synthesised[30], indicating that similar to muscarinic receptors, opioid receptors can be modulated by steroids. However, the non-genomic effects of steroids on the function of opioid receptors have not been studied in detail yet.

Various tissues differ in the content of membrane cholesterol. For example, cholesterol content is high in neurons and low in smooth muscle cells. Membrane cholesterol affects GPCR downstream signalling and may change the pharmacological profile of GPCR agonists[9]. Reduction of the content of membrane cholesterol attenuated signalling via δ-opioid receptors in neuronal cells but enhanced it in non-neuronal cells[31]. Thus, theoretically, natural variations in the interaction of receptors with membrane allow for achieving pharmacological selectivity based on variation in membrane composition among tissues resulting in tissue-specific selectivity.

In summary, membrane cholesterol binds to non-canonical sites at muscarinic and opioid receptors. Exploiting non-canonical cholesterol-binding sites and variations in the receptor-membrane interactions gives innovative pharmacotherapeutic opportunities including tissue-specific targeting.

Materials and Methods

Materials

Common chemicals were purchased from Sigma (Prague, CZ) in the highest available purity. Radiolabelled [^{35}S]GTPγS was Perkin Elmer NEG030H purchased from Lacomed (Kralupy nad Vltavou, CZ).

Cell culture and membrane preparation

Chinese hamster ovary cells were transfected with the genes of individual human variants of muscarinic and opioid receptors (Missouri S&T cDNA Resource Center, Rolla, MO, USA). CHO cell cultures were prepared as described previously. Stable cell lines were grown to confluence in 75 cm^2 flasks in Dulbecco's modified Eagle's medium supplemented with 10% fetal bovine serum and 2 million cells were subcultured in 100 mm Petri dishes. The medium was supplemented with 5 mM butyrate for the last 24 hours of cultivation to increase receptor expression. Cells were detached by mild trypsinization on day 5 after subculture. For cultivation of transiently transfected cells see "Construction of mutant receptors" below. Detached cells were washed twice in 50 ml of phosphate-buffered saline and 3 min centrifugation at 250 x g. Harvested cells were stored at -20°C overnight. Thawed cells were suspended in 20 ml of ice-cold incubation medium (100 mM NaCl, 20 mM Na-HEPES, 10 mM -$MgCl_2$, pH 7.4) supplemented with 10 mM EDTA and homogenized on ice by two 30-s strokes using a Polytron homogenizer (Ultra-Turrax; Janke & Kunkel GmbH & Co. KG, IKA-Labortechnik,

Staufen, Germany) with a 30 s pause between strokes. Cell homogenates were centrifuged for 5 min at 1000×g to remove whole cells and cell nuclei. The resulting supernatants were centrifuged for 30 min at 30,000×g. Pellets were suspended in a fresh incubation medium, incubated on ice for 30 min, and centrifuged again. The resulting membrane pellets were kept at -80 °C until assayed within 10 weeks.

Depletion of membrane cholesterol

The level of membrane cholesterol was decreased by incubation of whole detached cells in Krebs-HEPES buffer (KHB; final concentrations in mM: NaCl 138; KCl 4; $CaCl_2$ 1.3; $MgCl_2$ 1; NaH_2PO_4 1.2; Hepes 20; glucose 10; pH adjusted to 7.4) supplemented with 10 mM methyl-β-cyclodextrin (MβCD) at 37ºC for 30 min. The concentration of the cells in suspension was 20 million cells per ml. After incubation, the medium was removed and cells were washed twice with a triple incubation volume of fresh KHB.

Construction of mutant receptors

Plasmids coding muscarinic and opioid receptors were obtained from Missouri S&T cDNA Resource Center (Rolla, MO, USA) and used to generate sequences with the desired amino acid substitution using Q5 Site-Directed Mutagenesis Kit (NEB, via BioTek, Praha, Czech Republic). Primers were designed using NEBaseChanger (https://nebasechanger.neb.com/). CHO-K1 cells were transfected with desired plasmids using linear polyethylenimine (PEI) (Polysciences, Germany). Approximately 2 million cells were seeded in 10 ml of 1:1 mixture of Dulbeco's modified Eagle's and Ham's F-12 with L-glutamine in a 100 mm Petri dish and incubated for 24 hours at 37°C in a humidified 5% CO_2 atmosphere. DNA and PEI were mixed in a 1:3 ratio (12 ug DNA per 1 ml PBS : 36 ug PEI per 1 ml PBS) and incubated at room temperature for 30 min. Then 1 ml of transfection mix was added to a dish and incubated for 16 hours at 37°C in humidified 5% CO_2 atmosphere, Then DMEM was removed and 8 ml of fresh DMEM was added and cells incubated for additional 24 hours.

[^{35}S]GTPγS binding

Measurement of [^{35}S]GTPγS binding was carried out on membranes in 96-well plates at 30°C in the incubation medium described above supplemented with freshly prepared dithiothreitol at a final concentration of 1 mM, essentially as described by [9]. Membranes at concentrations of 10 µg of protein per well were used. The final volume was 200 µl, the final concentration of [^{35}S]GTPγS was 500 pM and the final concentration of GDP was 50 µM. Non-specific binding was determined in the presence of 1 µM unlabelled GTPγS. Total GTP binding capacity was determined in the absence of GDP. Agonist was added 15 min before [^{35}S]GTPγS. Incubation with [^{35}S]GTPγS was carried out for 20 min and the free ligand was removed by filtration through GF/C glass-fibre filtration plates (Millipore or Unifiletr) using a Brandel cell harvester (Brandel, Gaithersburg, MD, USA). Filtration and washing with ice-cold water lasted for 9 s. Filters were dried and then 40 µl of liquid scintillator Rotiszint was added to each well. The filtration plates were counted in a Wallac-Microbeta scintillation counter.

Experimental data analysis

Experiments were independent. Functional assays were carried out in quadruplicates. After subtraction of non-specific binding, data were normalized to the total GTP binding capacity determined in each experiment. EC_{50} values were calculated as logarithms.

Parameters of a functional response were determined by fitting Eq. 1 to experimental data.

$$y=1+\frac{(E_{MAX}-1)x^{n_H}}{EC_{50}^{n_H}+x^{n_H}} \qquad \text{Eq. 1}$$

where y is the functional response at a concentration of tested compound x, E_{MAX} is the maximal response to the tested compound, EC_{50} is the concentration causing half-efficient concentration and n_H is the slope factor (Hill coefficient).

Molecular modelling

Preparation of receptor structure

Structures of the M_2 and M_4 muscarinic acetylcholine 3UON, 4MQS, 5DSG and 8FX5 and μ, κ and δ opioid 4DKL, 5C1M, 6B73, 4DJH, 6PT2 and 4EJ4, A_{2A} adenosine 5IU4 and β_2 adrenergic 3D4S receptors were downloaded from RCSB Protein Data Bank (https://www.rcsb.org/). Non-protein molecules (except ligands) and nanobody or hydrolase parts of protein were deleted, and the resulting receptor protein was processed in Maestro using Protein Preparation Wizard according to Sastry et al. guidelines[32].

Coarse-grained MD

The Martini force field[33] coarse-grain system consisting of the receptor immersed in a 20 nm x 20 nm patch of POPC (1-palmitoyl-2-oleoyl-sn-glycero-3-phosphocholine) membrane containing 30 % of cholesterol was created using CHARMM-GUI (charmm-gui.org)[34] Membrane-Builder[35] and Martini maker[36]. After minimization and equilibration of the system, 3 independent runs of 2 µs molecular dynamics using Gromacs 2018 were run[37].

Cholesterol re-docking

Molecules of cholesterol that associated with a receptor during coarse-grained MD (cgMD) were back-mapped onto receptor structure. The resulting complexes were minimized in YASARA[38] and the cholesterol molecule was re-docked using the YASARA implementation of AutoDock[39]. The binding site was defined as a 5 Å extension in all directions to the cholesterol molecule and the AutoDock local search method was employed. All resulting poses were re-scored in YASARA by energy-minimisation of ligand pose and AutoDock VINA's local search, confined closely to the original ligand pose. The top-scoring pose was taken for further evaluation.

Simulation of molecular dynamics

To evaluate cholesterol binding to the receptor and assess its interactions with the receptor and potential effects on ligand binding, conventional molecular dynamics (cMD) of cholesterol-receptor complexes was simulated using Desmond/GPU ver. 6.5[40], one cholesterol molecule per simulation. The simulated system consisted of the receptor-ligand-cholesterol complex in the POPC membrane in water and 0.15 M NaCl. The system was first relaxed by the standard Desmond protocol for membrane proteins and then 600 ns NPγT (Noose-Hover chain thermostat at 300 K, Martyna-Tobias-Klein barostat at 1.01325 bar, isotropic coupling, and Coulombic cutoff at 0.9 nm). The quality of molecular dynamics simulation was assessed by the Simulation Quality Analysis tools of Maestro and analysed by the Simulation Event Analysis tool. Ligand-receptor interactions were identified using the Simulation Interaction Diagram tool.

References

1. Hauser AS, Attwood MM, Rask-Andersen M, et al (2017) Trends in GPCR drug discovery: new agents, targets and indications. Nat Rev Drug Discov 16:829–842. https://doi.org/10.1038/nrd.2017.178

2. Gimpl G (2016) Interaction of G protein coupled receptors and cholesterol. Chem Phys Lipids 199:61–73. https://doi.org/10.1016/j.chemphyslip.2016.04.006

3. Jakubík J, El-Fakahany EE (2021) Allosteric Modulation of GPCRs of Class A by Cholesterol. Int J Mol Sci 22:1953. https://doi.org/10.3390/ijms22041953

4. Li H, Papadopoulos V (1998) Peripheral-type benzodiazepine receptor function in cholesterol transport. Identification of a putative cholesterol recognition/interaction amino acid sequence and consensus pattern. Endocrinology 139:4991–7. https://doi.org/10.1210/endo.139.12.6390

5. Baier CJ, Fantini J, Barrantes FJ (2011) Disclosure of cholesterol recognition motifs in transmembrane domains of the human nicotinic acetylcholine receptor. Sci Rep 1:69. https://doi.org/10.1038/srep00069

6. Hanson MA, Cherezov V, Griffith MT, et al (2008) A specific cholesterol binding site is established by the 2.8 A structure of the human beta2-adrenergic receptor. Structure 16:897–905. https://doi.org/10.1016/j.str.2008.05.001

7. Taghon GJ, Rowe JB, Kapolka NJ, Isom DG (2021) Predictable cholesterol binding sites in GPCRs lack consensus motifs. Structure 29:499-506.e3. https://doi.org/10.1016/j.str.2021.01.004

8. Ballesteros JA, Weinstein H (1995) Integrated methods for the construction of three dimensional models and computational probing of structure function relations in G protein-coupled receptors. In: Sealfon SC, Conn PM (eds) Methods in Neurosciences. Academic Press, San Diego, CA, pp 366–428

9. Randáková A, Dolejší E, Rudajev V, et al (2018) Role of membrane cholesterol in differential sensitivity of muscarinic receptor subtypes to persistently bound xanomeline. Neuropharmacology 133:129–144. https://doi.org/10.1016/j.neuropharm.2018.01.027

10. Segala E, Guo D, Cheng RKY, et al (2016) Controlling the Dissociation of Ligands from the Adenosine A2A Receptor through Modulation of Salt Bridge Strength. J Med Chem 59:6470–9. https://doi.org/10.1021/acs.jmedchem.6b00653

11. Manglik A, Kruse AC, Kobilka TS, et al (2012) Crystal structure of the μ-opioid receptor bound to a morphinan antagonist. Nature 485:321–326. https://doi.org/10.1038/nature10954

12. Huang W, Manglik A, Venkatakrishnan AJ, et al (2015) Structural insights into μ-opioid receptor activation. Nature 524:315–321. https://doi.org/10.1038/nature14886

13. Che T, Majumdar S, Zaidi SA, et al (2018) Structure of the Nanobody-Stabilized Active State of the Kappa Opioid Receptor. Cell 172:55-67.e15. https://doi.org/10.1016/j.cell.2017.12.011

14. Claff T, Yu J, Blais V, et al (2019) Elucidating the active δ-opioid receptor crystal structure with peptide and small-molecule agonists. Sci Adv 5:eaax9115. https://doi.org/10.1126/sciadv.aax9115

15. Thal DM, Sun B, Feng D, et al (2016) Crystal structures of the M1 and M4 muscarinic acetylcholine receptors. Nature 531:335–340. https://doi.org/10.1038/nature17188

16. Maeda S, Qu Q, Robertson MJ, et al (2019) Structures of the M1 and M2 muscarinic acetylcholine receptor/G-protein complexes. Science 364:552–557. https://doi.org/10.1126/science.aaw5188

17. Levitt ES, Clark MJ, Jenkins PM, et al (2009) Differential effect of membrane cholesterol removal on μ- and δ-opioid receptors. A parallel comparison of acute and chronic signaling to adenylyl cyclase. Journal of Biological Chemistry 284:22108–22122. https://doi.org/10.1074/jbc.M109.030411

18. Liste MJV, Caltabiano G, Ward RJ, et al (2015) The molecular basis of oligomeric organization of the human M3 muscarinic acetylcholine receptor. Mol Pharmacol 87:936–53. https://doi.org/10.1124/mol.114.096925

19. Dolejší E, Chetverikov N, Szánti-Pintér E, et al (2021) Neuroactive steroids, WIN-compounds and cholesterol share a common binding site on muscarinic acetylcholine receptors. Biochem Pharmacol 192:114699. https://doi.org/10.1016/j.bcp.2021.114699

20. Daniel JM, Hulst JL, Lee CD (2005) Role of hippocampal M2 muscarinic receptors in the estrogen-induced enhancement of working memory. Neuroscience 132:57–64. https://doi.org/10.1016/j.neuroscience.2005.01.002

21. Horishita T, Minami K, Uezono Y, et al (2005) The effects of the neurosteroids: pregnenolone, progesterone and dehydroepiandrosterone on muscarinic receptor-induced responses in Xenopus oocytes expressing M1 and M3 receptors. Naunyn Schmiedebergs Arch Pharmacol 371:221–8. https://doi.org/10.1007/s00210-005-1022-1

22. Dolejší E, Szánti-Pintér E, Chetverikov N, et al (2021) Neurosteroids and steroid hormones are allosteric modulators of muscarinic receptors. Neuropharmacology 199:108798. https://doi.org/10.1016/j.neuropharm.2021.108798

23. Pallarés M, Darnaudéry M, Day J, et al (1998) The neurosteroid pregnenolone sulfate infused into the nucleus basalis increases both acetylcholine release in the frontal cortex or amygdala and spatial memory. Neuroscience 87:551–8. https://doi.org/10.1016/s0306-4522(98)00174-2

24. Darnaudéry M, Koehl M, Piazza PV, et al (2000) Pregnenolone sulfate increases hippocampal acetylcholine release and spatial recognition. Brain Res 852:173–9. https://doi.org/10.1016/s0006-8993(99)01964-2

25. Konar A, Shah N, Singh R, et al (2011) Protective role of Ashwagandha leaf extract and its component withanone on scopolamine-induced changes in the brain and brain-derived cells. PLoS One 6:e27265. https://doi.org/10.1371/journal.pone.0027265

26. Konar A, Gupta R, Shukla RK, et al (2019) M1 muscarinic receptor is a key target of neuroprotection, neuroregeneration and memory recovery by i-Extract from Withania somnifera. Sci Rep 9:13990. https://doi.org/10.1038/s41598-019-48238-6

27. André A, Gaibelet G, Le Guyader L, et al (2008) Membrane partitioning of various delta-opioid receptor forms before and after agonist activations: the effect of cholesterol. Biochim Biophys Acta 1778:1483–92. https://doi.org/10.1016/j.bbamem.2008.03.017

28. Ratka A, Hochhaus G, Wissler RN, Simpkins JW (1991) cAMP accumulation in opioid-sensitive SH-SY5Y neuroblastoma cells is modified by estradiol and progesterone. Mol Cell Endocrinol 78:155–62. https://doi.org/10.1016/0303-7207(91)90118-c

29. Schwarz S, Pohl P (1994) Steroids and opioid receptors. J Steroid Biochem Mol Biol 48:391–402. https://doi.org/10.1016/0960-0760(94)90080-9

30. McFadyen IJ, Houshyar H, Liu-Chen LY, et al (2000) The steroid 17alpha-acetoxy-6-dimethylaminomethyl-21-fluoro-3-ethoxy-pregna-3, 5-dien-20-one (SC17599) is a selective mu-opioid agonist: implications for the mu-opioid pharmacophore. Mol Pharmacol 58:669–76. https://doi.org/10.1124/mol.58.4.669

31. Huang P, Xu W, Yoon S-I, et al (2007) Cholesterol reduction by methyl-beta-cyclodextrin attenuates the delta opioid receptor-mediated signaling in neuronal cells but enhances it in non-neuronal cells. Biochem Pharmacol 73:534–49. https://doi.org/10.1016/j.bcp.2006.10.032

32. Sastry GM, Adzhigirey M, Day T, et al (2013) Protein and ligand preparation: parameters, protocols, and influence on virtual screening enrichments. J Comput Aided Mol Des 27:221–34. https://doi.org/10.1007/s10822-013-9644-8

33. Marrink SJ, Risselada HJ, Yefimov S, et al (2007) The MARTINI force field: coarse grained model for biomolecular simulations. J Phys Chem B 111:7812–24. https://doi.org/10.1021/jp071097f

34. Jo S, Kim T, Iyer VG, Im W (2008) CHARMM-GUI: a web-based graphical user interface for CHARMM. J Comput Chem 29:1859–65. https://doi.org/10.1002/jcc.20945

35. Wu EL, Cheng X, Jo S, et al (2014) CHARMM-GUI Membrane Builder toward realistic biological membrane simulations. J Comput Chem 35:1997–2004. https://doi.org/10.1002/jcc.23702

36. Qi Y, Ingólfsson HI, Cheng X, et al (2015) CHARMM-GUI Martini Maker for Coarse-Grained Simulations with the Martini Force Field. J Chem Theory Comput 11:4486–94. https://doi.org/10.1021/acs.jctc.5b00513

37. Abraham MJ, Murtola T, Schulz R, et al (2015) GROMACS: High performance molecular simulations through multi-level parallelism from laptops to supercomputers. SoftwareX 1–2:19–25. https://doi.org/10.1016/J.SOFTX.2015.06.001

38. Krieger E, Koraimann G, Vriend G (2002) Increasing the precision of comparative models with YASARA NOVA--a self-parameterizing force field. Proteins 47:393–402

39. Trott O, Olson AJ (2010) AutoDock Vina: improving the speed and accuracy of docking with a new scoring function, efficient optimization, and multithreading. J Comput Chem 31:455–61. https://doi.org/10.1002/jcc.21334

40. Shaw DE (2005) A fast, scalable method for the parallel evaluation of distance-limited pairwise particle interactions. J Comput Chem 26:1318–28. https://doi.org/10.1002/jcc.20267

Acknowledgements

We thank Prof. Esam El-Fakahany, University of Minnesota and Dr. Vladimir Dolezal, Institute of Physiology CAS for the critical reading of the manuscript. This work was supported by project National Institute for Neurological Research (Programme EXCELES, ID Project No. LX22NPO5107)—Funded by the European Union—Next Generation EU and Czech Academy of Sciences institutional support [RVO:67985823]. Access to computing and storage facilities owned by parties and projects contributing to the Czech National Grid Infrastructure MetaCentrum provided under the programme “Projects of Large Research, Development, and Innovations Infrastructures” (CESNET LM2015042) is appreciated.

Author contributions

N.C. constructed mutants and performed measurements of functional responses. A.R. contributed to measurements of functional responses and data analysis. D.N. contributed to molecular modelling and measurements of functional response. J.J. conceived the experimental design, secured financing, performed molecular modelling and data analysis and finalized the manuscript. All authors contributed to the manuscript preparation and approved the final version.

Competing interests

The authors declare no competing interests.

Supplementary Information: Cholesterol differentially modulates the activity of opioid and muscarinic receptors via common non-canonical binding site

Nikolai Chetverikov, Alena Janoušková-Randáková, Dominik Nelic, and Jan Jakubík*
Institute of Physiology CAS, Prague, Czech Republic
*, corresponding author, jan.jakubik@fgu.cas.cz

Supplementary Figures

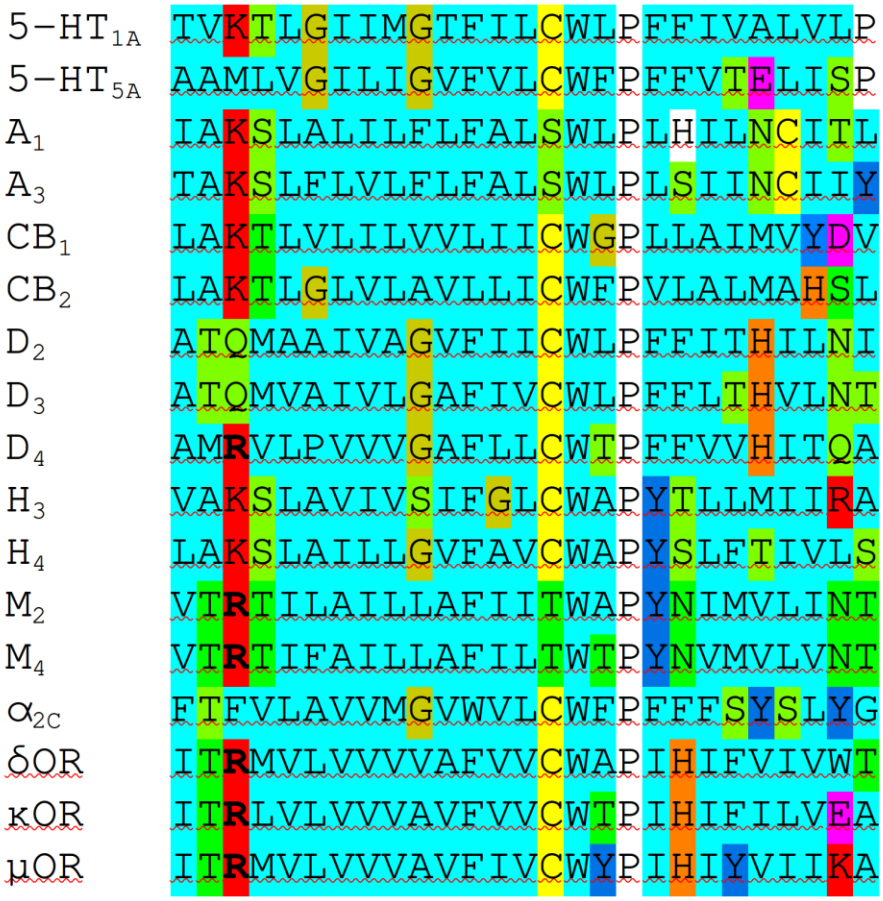

Figure S1 - Protein sequences of TM6
Aligned protein sequences of the sixth transmembrane α-helix (TM6) of selected $G_{i/o}$ coupled GPCRs of class A. Cyan, non-polar; green, polar; turquoise, aromatic polar; yellow, cysteine; gold, glycine; white, proline; magenta, acidic; red, basic amino acids. Bold, arginine.

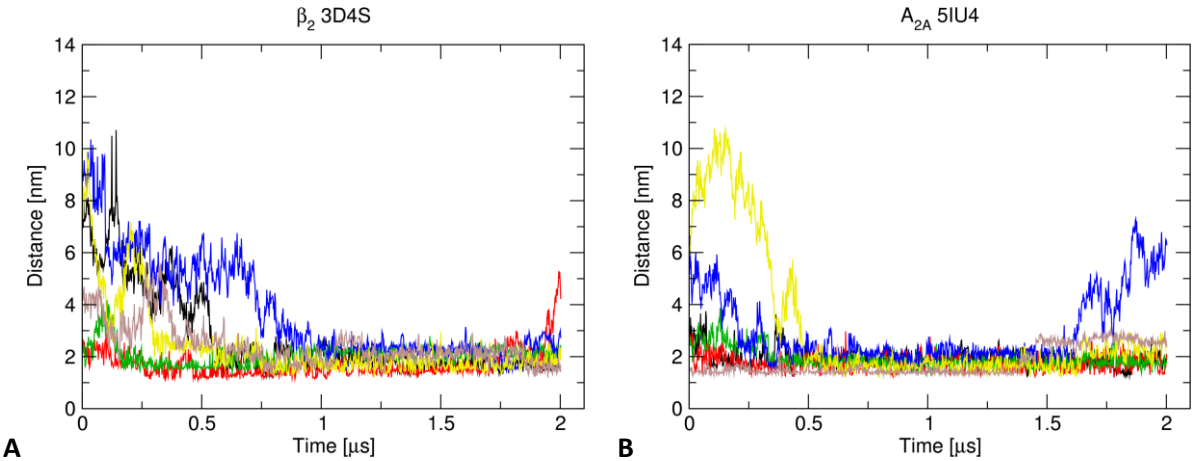

Figure S2 - Association of cholesterol with the β_2-adrenergic and A_{2A}-adenosine receptor

***A**, association trajectories of six cholesterol molecules with the β_2-adrenergic receptor in an inactive conformation (PDB code: 3D4S). **B**, association trajectories of six cholesterol molecules with A_{2A}-adenosine receptor in an inactive conformation (PDB code: 5IU4). X-axis, duration of coarse-grained MD in µs. Y-axis, the distance of the centre of cholesterol molecule from the centre of the receptor. Data are representative of one out of three independent MD simulations.*

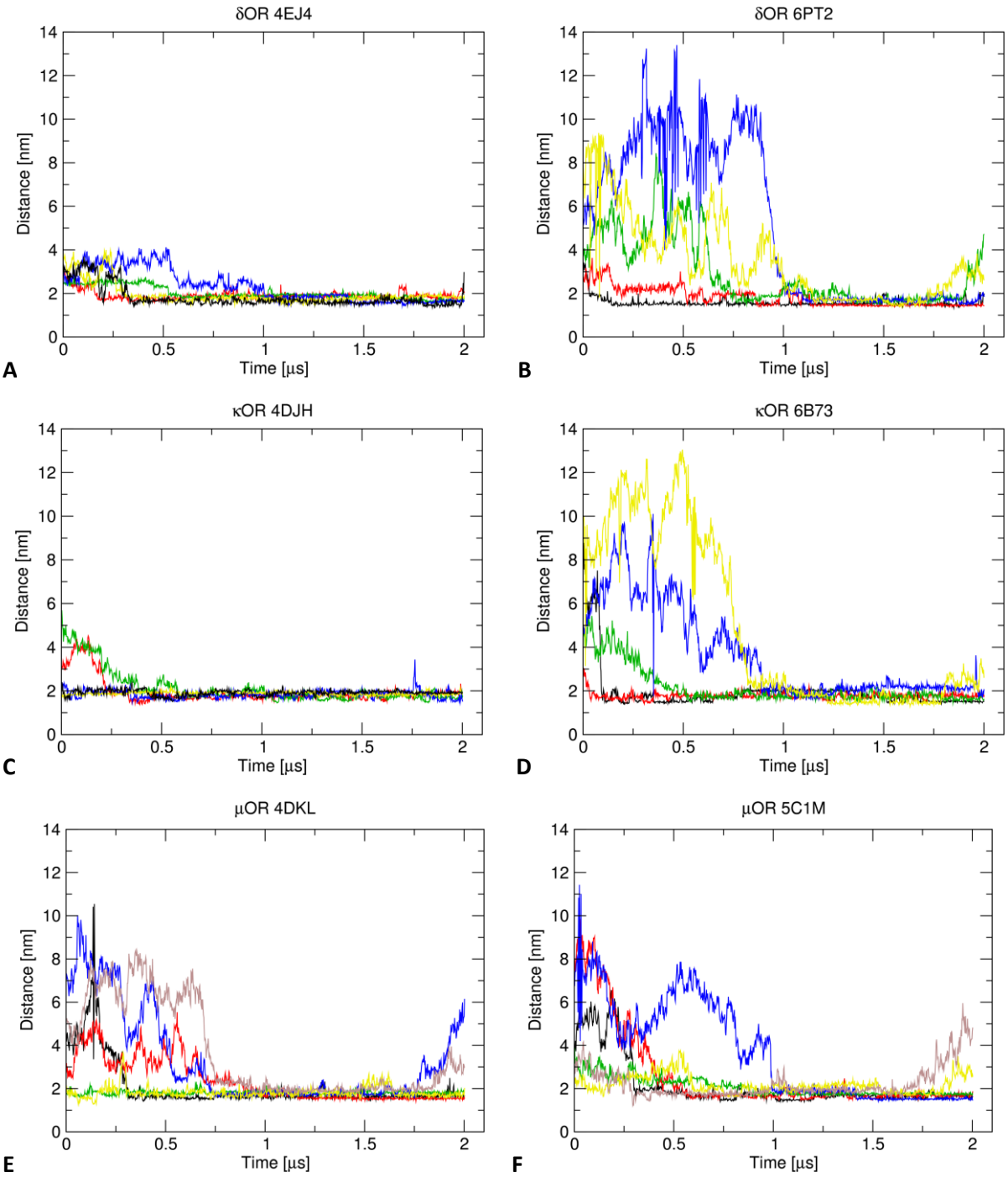

Figure S3 - Association of cholesterol with opioid receptors

*Association trajectories of five cholesterol molecules with the δ-opioid receptor in an inactive conformation (PDB code: 4EJH) (**A**) and an active conformation (PDB code: 6PT2) (**B**), the κ-opioid receptor in an inactive conformation (PDB code: 4EJH) (**C**) and in an active conformation (PDB code: 6PT2) (**D**), and the μ-opioid receptor in an inactive conformation (PDB code: 4EJH) (**E**) and an active conformation (PDB code: 6PT2) (**F**). X-axis, duration of coarse-grained MD in μs. Y-axis, the distance of the centre of cholesterol molecule from the centre of the receptor. Data are representative of one out of three independent MD simulations.*

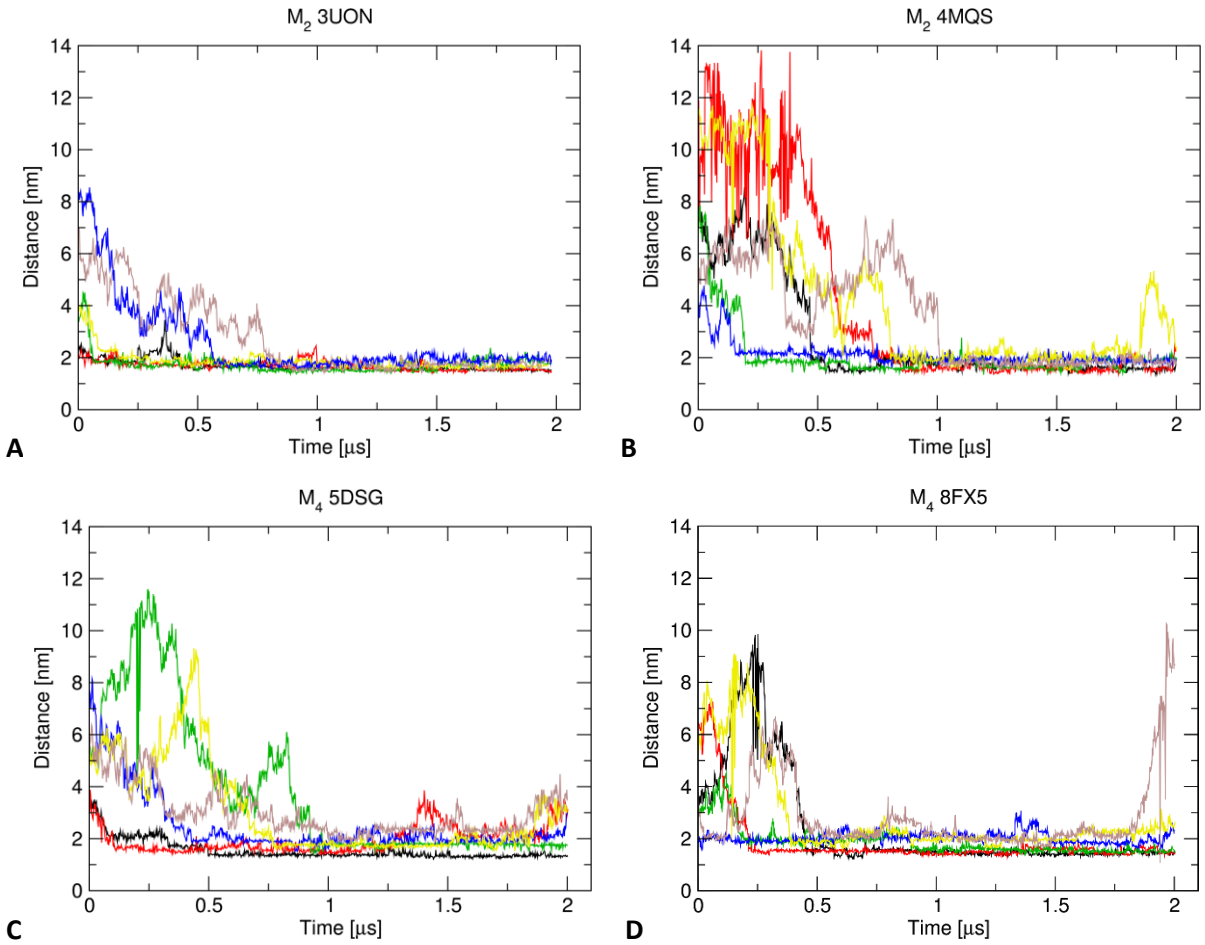

Figure S4 - Association of cholesterol with muscarinic receptors

*Association trajectories of six cholesterol molecules with M_2-muscarinic receptor in an inactive conformation (PDB code: 3UON) (**A**) and an active conformation (PDB code: 4MQS) (**B**) and M_4-muscarinic receptor in an inactive conformation (PDB code: 5DSG) (**C**) and an active conformation (PDB code> 8FX5) (**D**). X-axis, duration of coarse-grained MD in µs. Y-axis, the distance of the centre of cholesterol molecule from the centre of the receptor. Data are representative of one out of three independent MD simulations.*

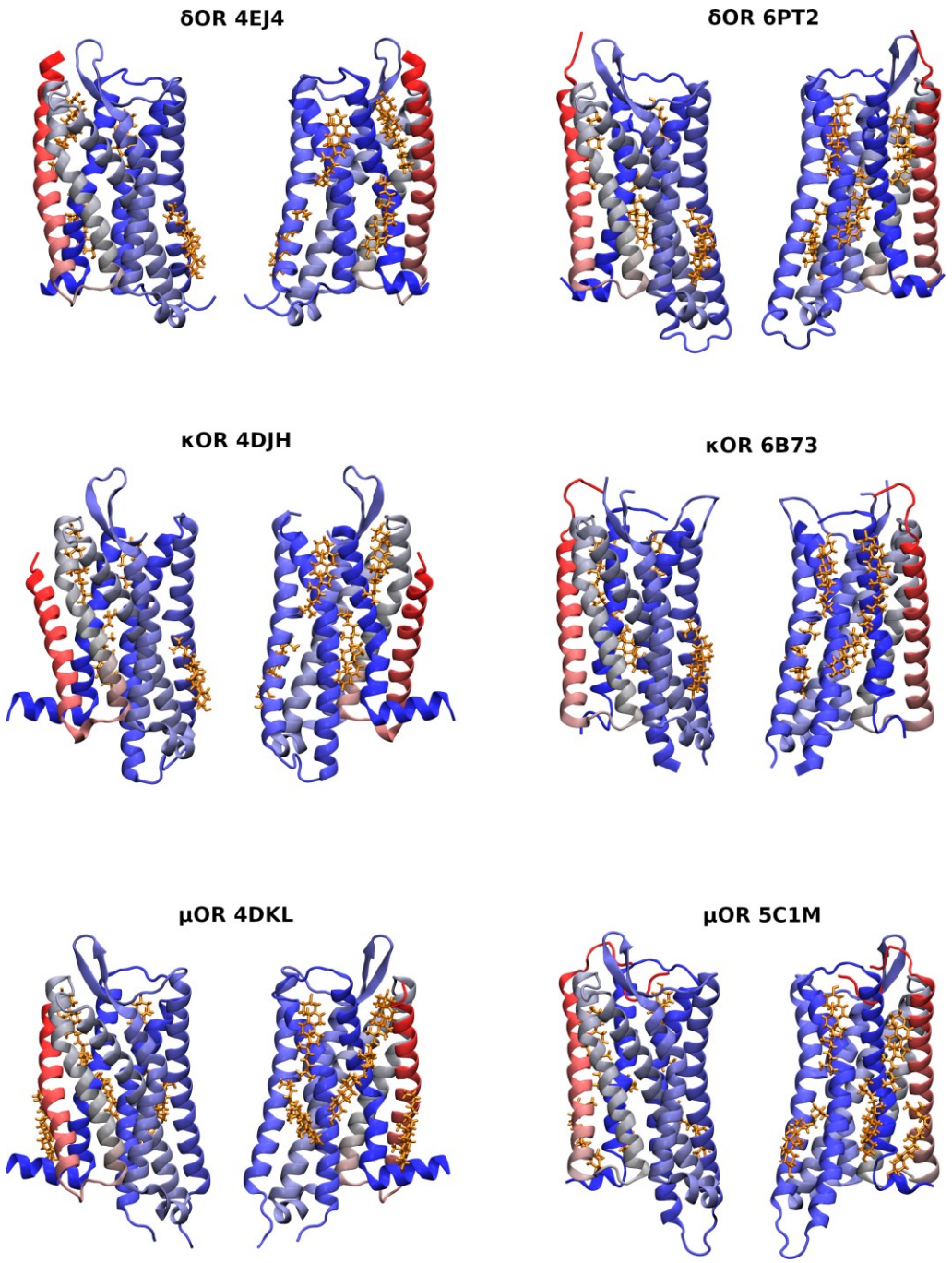

Figure S5 - Cholesterol binding to opioid receptors

Molecules of cholesterol that associated with opioid and muscarinic receptors in an inactive or active conformation during cgMD were back-mapped and re-docked to the receptors. Cholesterol is gold. The receptor is in a red-grey-blue gradient. Orientation: extracellular up, TM3 (left) or TM6 (right) in front.

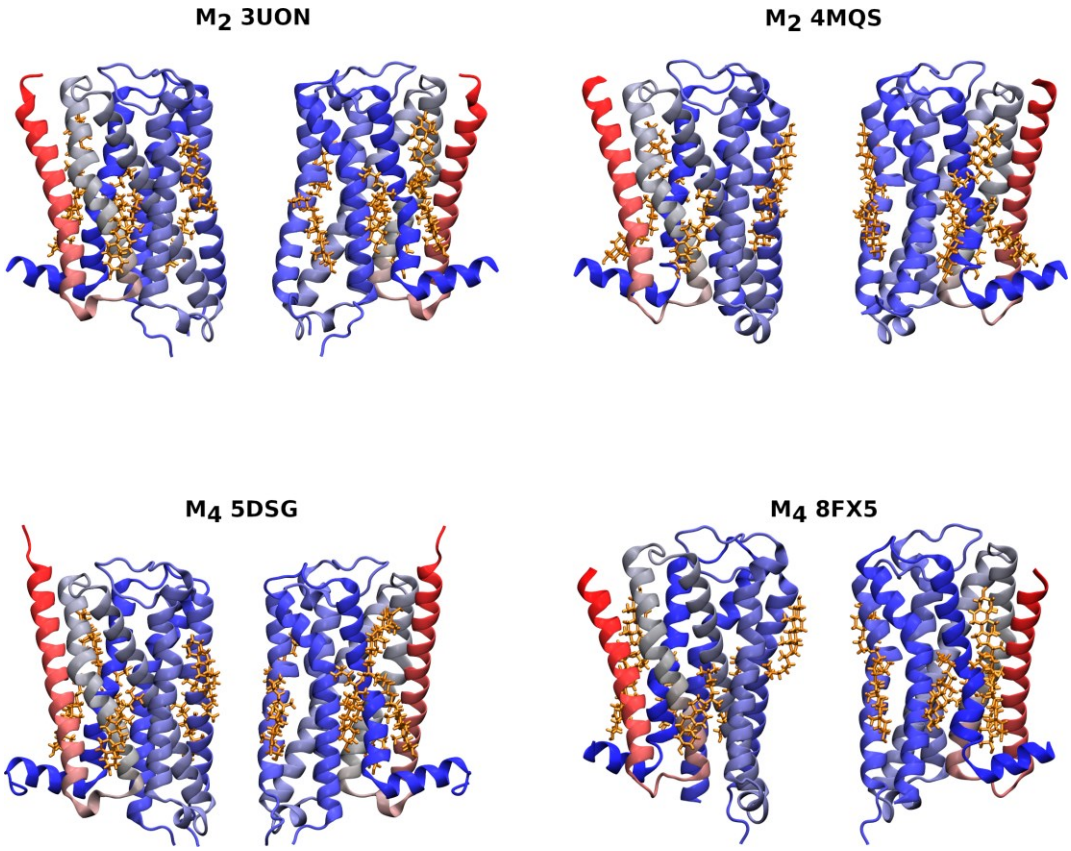

Figure S6 - Cholesterol binding to muscarinic receptors

Molecules of cholesterol that associated with opioid and muscarinic receptors in an inactive or active conformation during cgMD were back-mapped and re-docked to the receptors. Cholesterol is gold. The receptor is in a red-grey-blue gradient. Orientation: extracellular up, TM3 (left) or TM6 (right) in front.

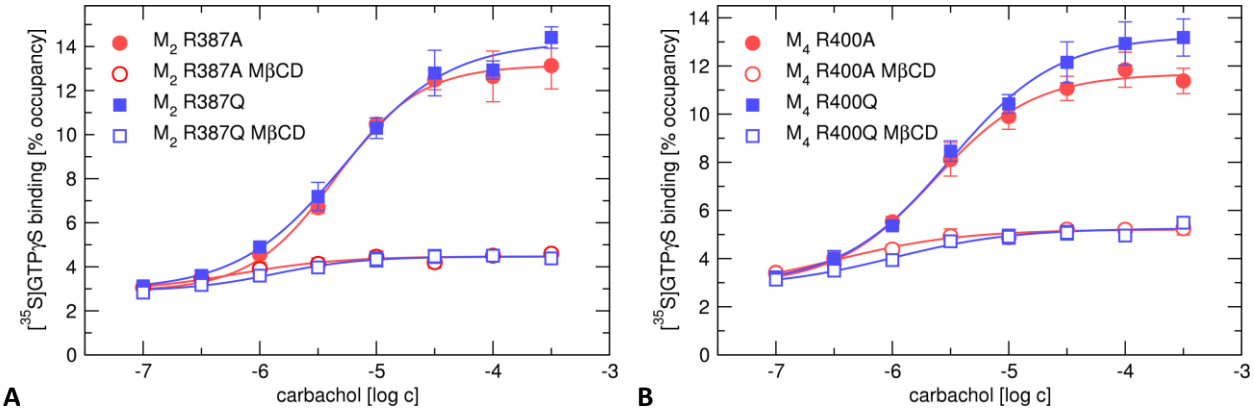

Figure S7 -Effects of cholesterol depletion on functional response of mutated muscarinic receptors

Effects of membrane-cholesterol depletion (open symbols) on functional responses of mutated (red circles - $R^{6.35}$ to alanine; blue squares – $R^{6.35}$ to glutamine) M_2- (left) and M_4-muscarinic (right) receptors to carbachol. Ordinate, [^{35}S]GTPγS binding is expressed as % of occupancy of G-protein binding sites. Abscissa, the concentration of agonist is expressed as a decadic logarithm of molar concentration. Data are means ± SD from 3 independent experiments performed in quadruplicates.

Supplementary Tables

Table S1 Parameters of functional response to agonists at native and methyl-β-cyclodextrin-treated (MβCD) membranes.

EC_{50} values are expressed as negative decadic logarithms. E_{MAX} and basal values are expressed as % of occupancy of G-protein binding sites. Data are means ± SD from 3 independent experiments performed in quadruplicates.

	pEC_{50}			E_{MAX} [% occupancy]			Basal [% occupancy]		
δ-OR	7.87	±	0.08	10.65	±	0.38	1.92	±	0.07
δ-OR MβCD	7.86	±	0.02	7.35	±	0.07*	1.68	±	0.06*
κ-OR	4.82	±	0.06	10.1	±	0.29	2.5	±	0.08
κ-OR MβCD	4.57	±	0.05*	5.27	±	0.11*	2.4	±	0.08
μ-OR	7.75	±	0.05	11.55	±	0.28	2.09	±	0.07
μ-OR MβCD	7.89	±	0.07*	9.38	±	0.31*	1.18	±	0.05*
M_2	5.04	±	0.04	12.14	±	0.26	2.46	±	0.08
M_2 MβCD	5.23	±	0.04*	14.97	±	0.25*	2.9	±	0.09*
M_4	5.28	±	0.07	11.13	±	0.35	2.46	±	0.08
M_4 MβCD	5.72	±	0.02*	13.19	±	0.10*	2.9	±	0.09*

**, different from untreated (P<0.05, paired t-test)*

Table S2 Parameters of functional response to agonists at wild type ($R^{6.35}$) and mutated receptors.

EC_{50} values are expressed as negative decadic logarithms. E_{MAX} and basal values are expressed as % of occupancy of G-protein binding sites. Data are means ± SD from 3 independent experiments performed in quadruplicates.

	pEC_{50}			E_{MAX} [% occupancy]			basal [% occupancy]		
δ-OR $R^{6.35}$	7.55	±	0.09	10.75	±	0.58	1.92	±	0.05
δ-OR $A^{6.35}$	7.45	±	0.08	10.28	±	0.77	1.70	±	0.04*
δ-OR $Q^{6.35}$	7.37	±	0.07	9.07	±	0.99	1.68	±	0.04*
κ-OR $R^{6.35}$	5.28	±	0.02	9.56	±	0.79	2.50	±	0.07
κ-OR $A^{6.35}$	6.01	±	0.02*	5.03	±	0.27*	2.40	±	0.05
κ-OR $Q^{6.35}$	6.05	±	0.03*	6.75	±	0.49*	2.41	±	0.09
μ-OR $R^{6.35}$	7.75	±	0.09	11.61	±	1.35	2.09	±	0.08
μ-OR $A^{6.35}$	7.82	±	0.05	12.75	±	1.77	1.54	±	0.07*
μ-OR $Q^{6.35}$	7.64	±	0.06	7.92	±	1.01*	1.18	±	0.04*
M_2 $R^{6.35}$	5.05	±	0.03	12.16	±	0.10	2.46	±	0.07
M_2 $A^{6.35}$	5.26	±	0.05*	13.47	±	0.36*	2.89	±	0.10*
M_2 $Q^{6.35}$	5.23	±	0.03*	14.29	±	0.78*	2.90	±	0.09*
M_4 $R^{6.35}$	5.32	±	0.01	10.59	±	0.13	2.46	±	0.08
M_4 $A^{6.35}$	5.60	±	0.04*	11.79	±	0.08*	2.89	±	0.10*
M_4 $Q^{6.35}$	5.53	±	0.01*	13.28	±	0.69*	2.90	±	0.09*

**, different from wild type (P<0.05 after Bonferroni correction, paired t-test)*

Table S3 Parameters of functional response to agonists at mutated receptors.

EC_{50} values are expressed as negative decadic logarithms. E_{MAX} and basal values are expressed as % of occupancy of G-protein binding sites. Data are means ± SD from 3 independent experiments performed in quadruplicates.

	pEC_{50}			E_{MAX} [% occupancy]			basal [% occupancy]		
M_2 $A^{6.35}$	5.26	±	0.02	13.55	±	0.29	2.90	±	0.04
M_2 $A^{6.35}$ MβCD	6.17	±	0.03*	4.46	±	0.20*	2.88	±	0.04
M2 $Q^{6.35}$	5.26	±	0.02	14.07	±	1.01	2.94	±	0.01
M2 $Q^{6.35}$ MβCD	5.73	±	0.01*	4.50	±	0.22*	2.89	±	0.03
M4 $A^{6.35}$	5.64	±	0.02	11.71	±	0.93	2.89	±	0.04
M4 $A^{6.35}$ MβCD	6.50	±	0.02*	5.11	±	0.01*	2.71	±	0.02*
M4 $Q^{6.35}$	5.50	±	0.02	13.40	±	0.60	2.92	±	0.02
M4 $Q^{6.35}$ MβCD	5.89	±	0.02*	5.22	±	0.10*	2.82	±	0.02*

**, different from untreated (P<0.05, paired t-test)*